JOURNAL OF MATERIALS SCIENCE 23 (1988) 3137–3143

Effect of hydrogen exposures on the strength of sintered alpha silicon carbide

E. SAVRUN*, A. D. MILLER
Department of Materials Science and Engineering, University of Washington, Seattle, Washington, 98105, USA

The room-temperature strength distributions of sintered alpha silicon carbide (SASC) were determined for polished bars. The bars were broken in the as-polished condition after exposure to hydrogen only and after exposure to hydrogen under two different static stresses. The hydrogen exposures were at 1370° C for times up to 50 h. The strength distributions displayed a dependence on both the exposure time and the magnitude of the applied stress. In stressed exposures, the strength distributions were apparently controlled by competing mechanisms. Under the lower applied stress, the material was weaker than the as-polished control group, as was the material exposed to hydrogen with no stress applied. Under the higher applied stress, the material was stronger than the control group.

1. Introduction

The influence of the environment on the strength of structural materials is an extremely important factor that must be incorporated into the design of high-performance systems. The nature of the environment can influence, in a complicated way, the nature of the flaws which limit the strength of brittle materials. Therefore, understanding of the flaw behaviour in adverse environments is essential in the design and failure prediction of components.

Silicon carbide is one of the most promising ceramics under consideration for use in energy conversion applications. Potential structural applications include automotive gas turbine components [1], high-temperature heat exchangers [2] and thermonuclear reactors [3]. The limiting conditions for stability and structural integrity of SiC in these diverse environments must be established.

Since many of the potential applications of silicon carbide require resistance to highly oxidizing atmospheres at high temperatures, the effects of oxidation on the mechanical behaviours of a variety of silicon carbides have been extensively studied [4–11]. Easler [4] and Easler *et al.* [5] studied the effect of applied stress on the strength of sintered alpha silicon carbide during oxidation. They suggested that a static fatigue limit or a stress intensity threshold for slow crack extension could exist, and that flaw growth occurs for flaws greater than a critical size, but flaw blunting occurs for flaws smaller than the critical size.

Silicon carbide is also often used in hydrogen-containing environments, e.g. in the heater head of a Stirling engine, in the first wall of a nuclear fusion reactor, and in heat exchangers. Therefore, an understanding of the effects of hydrogen on the microstructure and properties of silicon carbide is essential for design purposes. However, the effects of hydrogen-containing environments on silicon carbide have received little attention. Horn *et al.* [12] claim that even though flowing steam at 1400° C resulted in a weight loss of 0.4 mg h^{-1}, the erosion rate of silicon carbide is unaffected by the presence of hydrogen in the steam. McKee and Chaterji [13] reported that hydrogen does not cause any corrosion in SiC at 900° C. Verghese *et al.* [14] and Causey *et al.* [15] report that the activation energy for hydrogen diffusion in silicon carbide is quite high, suggesting the possibility of some form of chemical bonding within the material. Fischman [16] supports this view, but neither work addresses the strength. The only work on the effect of hydrogen on the strength of silicon carbide appears to be that of Jero [17] which demonstrated that exposure to 40% hydrogen in argon at 1370° C causes rapid surface degradation and a reduction in the strength for exposure times as little as three hours.

Other than the cited studies, the effect of hydrogen on silicon carbide at high temperatures has been studied almost exclusively within the context of using hydrogen to etch single-crystal SiC for semiconductor applications [18–21].

This study is concerned with the room-temperature strength distribution of polished sintered alpha silicon carbide, and with the changes that occur in the distribution after various environmental exposures. The environments were hydrogen with no stress applied and with two different applied stresses. Exposure time was also varied.

2. Experimental procedure

2.1. Specimen preparation and characterization

The sintered alpha silicon carbide (Hexalloy SASC (1981), The Carborundum Co., Niagara Falls, New York) used in this study was purchased in the form of

*Present address: Photon Sciences, AMD, Bothell, Washington, 98111 USA.

0022–2461/88 $03.00 + .12

billets, each measuring 5.00 cm × 5.00 cm × 1.25 cm. The material contained small amounts of boron (~0.01%) and carbon (~0.3%) as densification aids, and had a density of 3.16 g cm^{-3}. Specimens were cut from billets using a diamond blade and ground, finishing with 600 grit B_4C powder, and finally were polished to a size of 0.27 cm × 0.27 cm × 3.0 cm, finishing with 1 μm diamond paste on four sides in the longitudinal direction. Edges were bevelled at 45° by grinding, finishing with 600 grit B_4C powder.

Strength distributions were determined by fracturing specimens in a four-point bend geometry with 1/3 point loading configuration. The outer span was 2.20 cm and the inner span was 0.73 cm. All strength tests were carried at a crosshead speed of 0.2 mm min^{-1} at room temperature. After fracture, the broken pieces were collected and stored in a desiccator for subsequent fractographic analyses.

2.2. Exposure to hydrogen

Specimens were exposed to hydrogen in a controlled-atmosphere cold-wall furnace equipped with a tungsten resistance heating element (Centorr Model 15-2x3T-22, Centorr Associates, Suncook, New Hampshire). During exposures, the specimens were placed inside a specially made SiC specimen holder in such a way that they were separated from each other with sintered alpha silicon carbide pins. All exposures were carried out in pure, dry hydrogen flowing at a rate of 1 cubic foot per hour (0.028 m^3 h^{-1}) at 1370° C. Zero-stress exposures were carried out for 1, 20, and 50 h while exposures under applied stress were for 1 to 20 h.

The specimens were loaded in a four-point bending configuration, with an outer span of 2.2 cm and an inner span of 1.1 cm, resulting in 1/4 point loading geometry. This geometry was selected to ensure that the room-temperature tests were performed within the constant stress region of the statically loaded specimens. A special dead-loading mechanism was incorporated into the furnace and loading was performed by using lead blocks. Loading and unloading were done as quickly as possible. Two different static stresses were applied so that the effect of stress level could be observed. After exposures to hydrogen, the specimens were stored in a desiccator until testing in flexure at room temperature.

2.3. Data analysis

The strength data were analysed using a two-parameter Weibull expression. The Weibull model and its applications have been described in detail by Bury [22], Davies [23] and Johnson [24]. The Weibull cumulative distribution function (CDF) was integrated over the surface area of the specimen, since all observed failures originated from the surface flaws. For the test geometry used in this study, the expression takes the form

$$F = 1 - \exp\left(-\frac{A\,(m+2)\,(m+3)}{12\,(m+1)^2}\right)\left(\frac{S}{S_0}\right)^m \quad (1)$$

where F is the probability of failure, A is the total surface area of specimen, S is the fracture strength, S_0 is a scaling parameter and m is the Weibull modulus. Values for F were calculated via order statistics, using the relation

$$F = \frac{n}{N+1} \quad (2)$$

where n is the serial number in order of strength and N is the total number of data points. A double-logarithmic transformation yields the linearized form of Equation 1:

$$\ln\ln\left(\frac{1}{1-F}\right) = m \ln S + m \ln\left(\frac{A\,(m+2)\,(m+3)}{12\,(m+1)^2\,S_0^m}\right) \quad (3)$$

A least-squares linear regression analysis was used to calculate the parameters m and S_0 in Equation 3. The correlation coefficient, R, was also calculated to estimate the goodness-of-fit of the data to the two-parameter Weibull model. Statistical analyses were performed on strength data to determine the statistical significance of the observed trends. A one-way analysis of variance was applied to the means of distributions to determine if they were statistically identical. If the means failed this test, the Student–Newman–Keuls (SNK) test was applied to pairs of means [25]. All comparisons were done at 95% confidence level.

3. Results and discussion

3.1. Material characterization

The microstructure of as-received material, shown in Fig. 1, was revealed after polishing and etching with Murakami's etchant. The average grain size was estimated to be 6 μm with a range from 4 to 10 μm, while pore size ranged from 5 to 30 μm. X-ray diffraction studies determined that the material had basically 6H polytype structure with small amounts of 4H polytype. Scanning Auger microprobe (SAM) studies showed the presence of free carbon, particularly at grain boundaries, and randomly distributed boron. These observations are in agreement with the data supplied by the manufacturer.

The strength data of as-polished specimens fit well into a two-parameter Weibull distribution with a modulus of 7.5 and an average strength of 426 MPa. This result is in agreement with that of other investigators [4, 5, 17]. Fractography showed that failures in as-polished specimens originated from surface or near-surface pores, or from subsurface flaws including pores, inclusions and loosely sintered regions which were produced during processing (Fig. 2).

3.2. Exposure to hydrogen

Scanning electron microscopy (SEM) investigations of the specimens exposed to hydrogen revealed severely altered surfaces. This surface degradation occurs, mainly, due to hydrogen attack on carbon-rich high-energy grain boundaries. Fig. 3 shows the extent to which the surface has changed after exposure. Note that the severity of the surface change increases with increasing exposure time. X-ray diffraction studies did not indicate any change in the material after exposures.

The strength distributions after exposure to

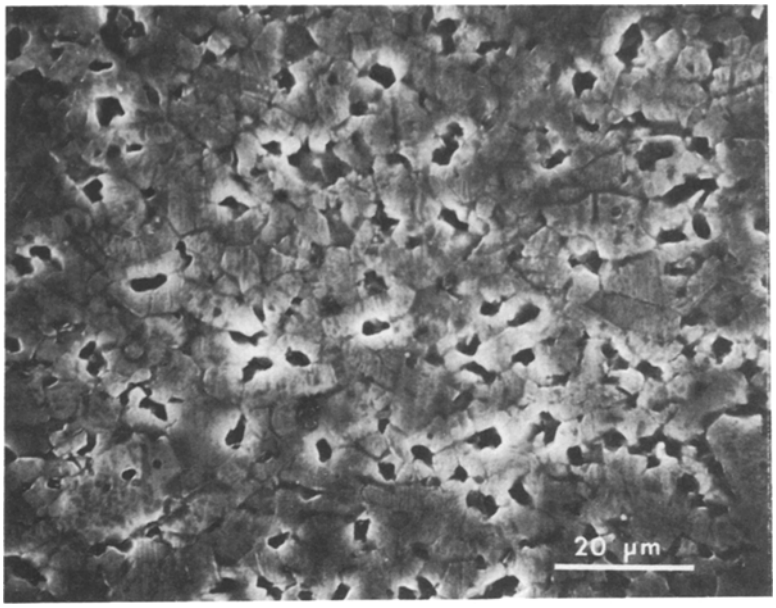

Figure 1 Microstructure of as-polished material. Etched with Murakami's solution.

hydrogen are compared to the as-polished strength distribution in Fig. 4. After one hour of exposure there is a loss in the strength across the entire distribution which becomes greater at longer exposure times. The average strengths and Weibull parameters for all distributions are summarized in Table I.

The Weibull modulus initially increased from 7.5 to 15 for one hour exposure, and then decreased to 11.4 and stayed about the same (at a value of 11) upon further exposures. The initial increase in the Weibull modulus compared to the control specimens suggests the development of a high-density population of flaws of severity equal to or sightly greater than those present in control specimens due to hydrogen–surface interactions. The average strength displayed a decreasing trend with increasing exposure times. It decreased from 426 to 376 MPa after 50 h, displaying a 12% decrease when compared to that of the as-polished group. Analysis of variance showed that average strengths were significantly different. The SNK test determined that $\bar{S}_0 = \bar{S}_1 \neq \bar{S}_{20} \neq \bar{S}_{50}$, where $\bar{S}$ is the average strength and subscripts refer to exposure times. Jero [17] observed a similar decreasing trend in the average strength in hydrogen at 1400° C. However, he claims a more severe strength reduction of 26% after 50 h exposures. This discrepancy in the degree of strength reduction is not considered significant since the small number of specimens used in each study, the fact that the specimens were from different lots, and different experimental procedures could easily cause the variation seen. What is significant is that both studies indicated a definite strength reduction under these conditions. Jero [17] also showed that exposure to pure dry argon at 1400° C for up to 50 h did not cause any significant strength reduction in sintered alpha silicon carbide.

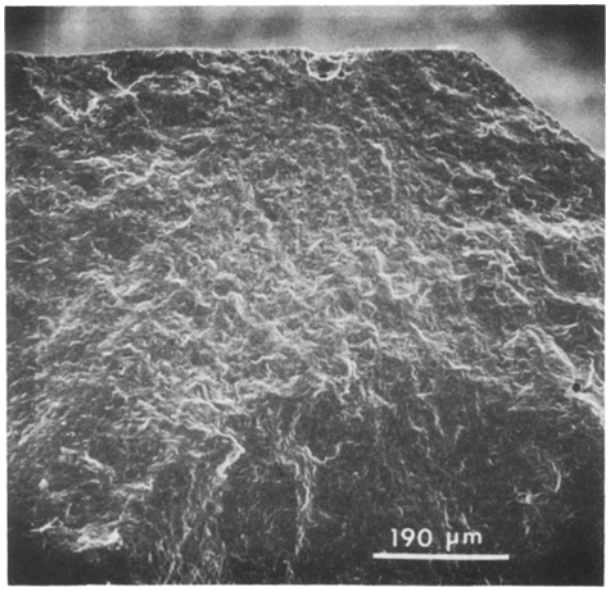

Figure 2 Scanning electron micrograph of the failure origin in an as-polished specimen: a surface pore on the tensile surface.

The decrease in average strength and Weibull modulus with time suggests an increase in the flaw size and a broadening of the flaw size distribution. This is consistent with a chemical reaction mechanism, the nucleation and growth of new flaws and an increase in the size of existing ones. Microscopic observations of exposed surfaces are consistent with this mechanism. Attack by hydrogen on the boundaries intersecting the pores would make the effective flaw size larger.

After zero-stress exposures, detailed fractographic studies showed that failures originated almost exclusively from the surface or near-surface pores located on tensile surfaces or edge sites, as shown in Fig. 5. This observation is the same as that on the as-polished group. Therefore, no obvious conclusions can be drawn on the effect of hydrogen on the nature of the strength controlling flaws.

3.3. Exposure to hydrogen under stress

The strength distributions after exposure to hydrogen under static stress are compared to those of zero-stress exposures for 1 h (Fig. 6a) and for 20 h (Fig. 6b).

After one hour of exposure under the lower applied stress (130 MPa), the strength distribution is nearly identical to that after zero-stress exposure, displaying almost the same amount of scatter. The Weibull modulus decreased from 15 to 12.5. Correlation coefficients of 0.97 indicate very good fits to the two-

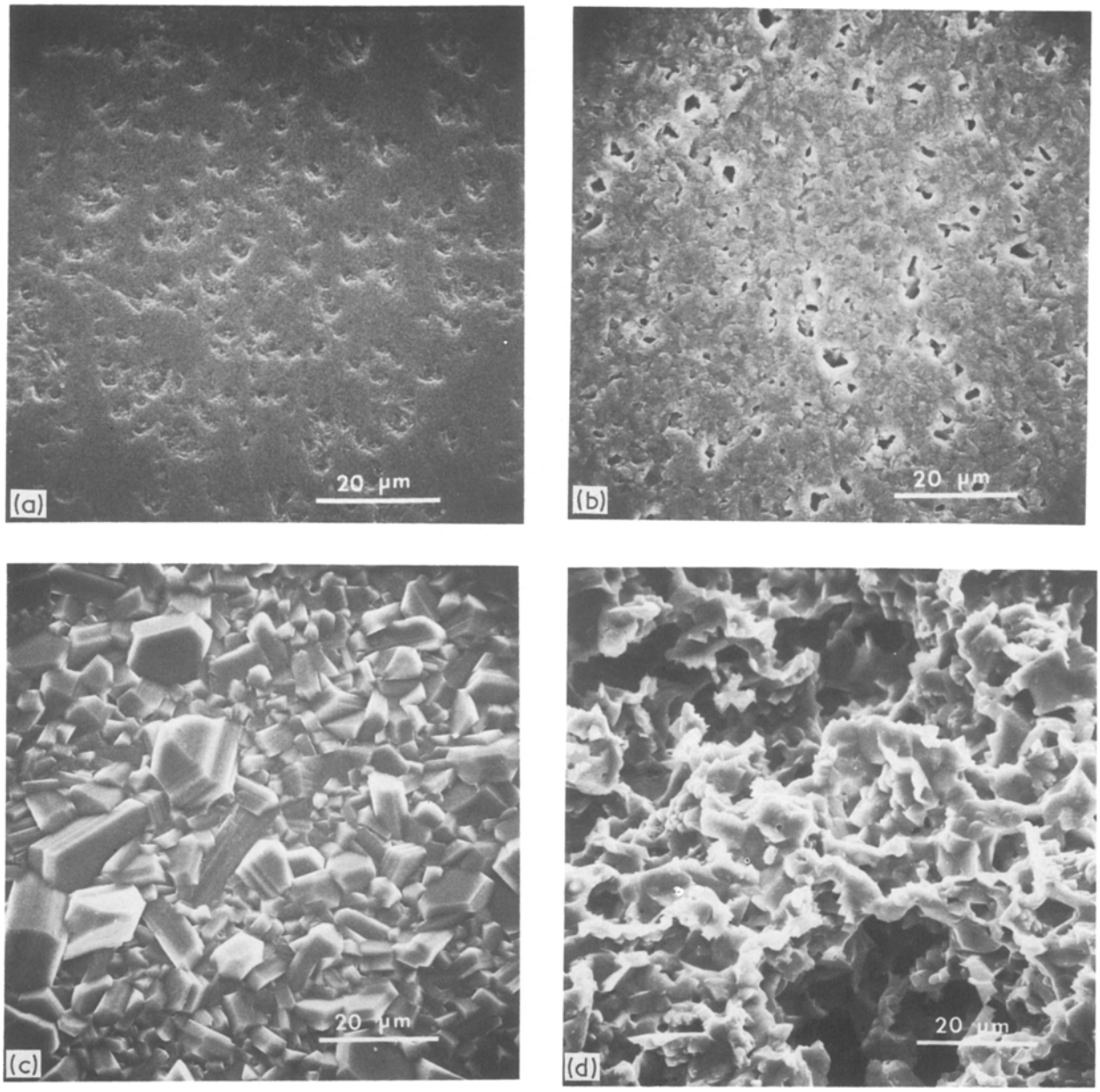

Figure 3 Scanning electron micrographs of specimen surfaces before and after exposures to hydrogen: (a) as-polished, (b) 1 h, (c) 20 h, (d) 50 h.

parameter Weibull distribution, for both cases. The average strength increased from 412 to 423 MPa. This indicates that the lower applied stress did not change the nature of the strength-controlling flaws in the material. Fractographic analysis did not show any particular change in the nature of the strength-controlling flaws. The failure sites were surface or near-surface pores.

The strength distribution after one hour of exposure under a higher static stress (265 MPa) displayed a rather different behaviour. It showed a transition at about 46% probability of failure corresponding to a strength of 536 MPa. The lower-strength portion of the distribution did not change, indicating that the applied stress did not affect the strength of a specimen in this region, while the upper portion of the

TABLE I Weibull parameters for distributions obtained after hydrogen exposure

Distribution set	No. of specimens	$\bar{S}$ (MPa)	m	S_0	R
As-polished	22	426 ± 59	7.5 ±0.2	452	0.99
1 h	15	412 ± 27	15.0 ±1.0	426	0.97
20 h	19	387 ± 32	11.4 ±0.5	403	0.97
50 h	18	376 ± 36	11.0 ±0.5	392	0.98
1 h, 130 MPa	15	423 ± 34	12.5 ±0.8	439	0.97
1 h, 265 MPa	14	431 ± 43	9.8 ±0.9	451	0.96
20 h, 130 MPa	18	392 ± 43	9.5 ±0.6	411	0.97
20 h, 265 MPa	21	436 ± 32	13.8 ±1.1	452	0.94

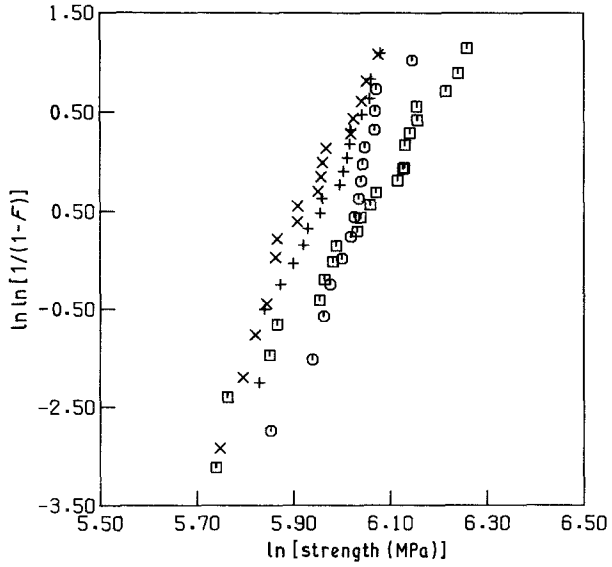

Figure 4 Linearized Weibull plot showing effect of different exposure times on the strength distribution of as-polished control group: (▣) control group, (◒) 1 h, (+) 20 h, (x) 50 h.

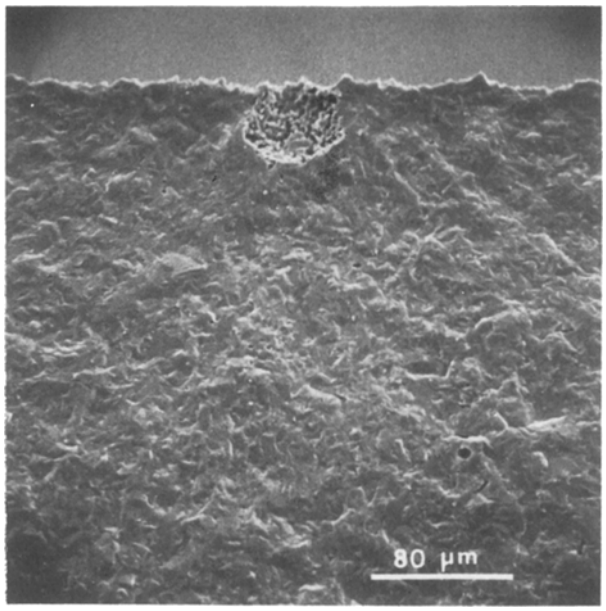

Figure 5 A typical failure origin after 20 h zero-stress exposure: a surface pore.

distribution shifted to higher strength levels, displaying a strengthening behaviour when compared to the corresponding zero-stress exposure strength distribution (Fig. 6a). The Weibull modulus was about 10, which is somewhat less when compared to that, 15, of the corresponding group without any applied stress. A correlation coefficient of 0.96 still indicates an excellent fit to the two-parameter Weibull model. Analysis of variance and SNK tests determined that the average strengths were statistically identical, $\bar{S}_0 = \bar{S}_{130} = \bar{S}_{265}$ where subscripts refer to applied stresses. These observations imply the presence of at least two competing mechanisms within the distribution. At higher failure probabilities (specimens with smaller flaws) strengthening is dominant. At lower failure probabilities (specimens with larger flaws) the effect of strengthening may be counterbalanced by a weakening mechanism, i.e. hydrogen reaction, thus showing no change in the strength.

After 20 h exposure under the lower applied stress (Fig. 6b) the strength distribution was nearly identical to that after zero-stress exposure, with the exception of the very upper end of the distribution which shifted to higher strengths at about 80% probability of failure and a strength of 403 MPa. Fig. 6b shows that the amount of scatter in both cases is nearly the same. The Weibull moduli were 11 for zero-stress exposure and 9.5 for exposure under the lower applied stress. Correlation coefficients of 0.97 for both cases indicate very good fits to the two-parameter Weibull distribution. The average strength did not change by more than 5 MPa. These observations indicate that there is not any significant stress effect on the strength distribution after 20 h exposure to hydrogen under 130 MPa static stress.

After 20 h exposure under the higher applied stress (265 MPa), the strength distribution shifted to higher

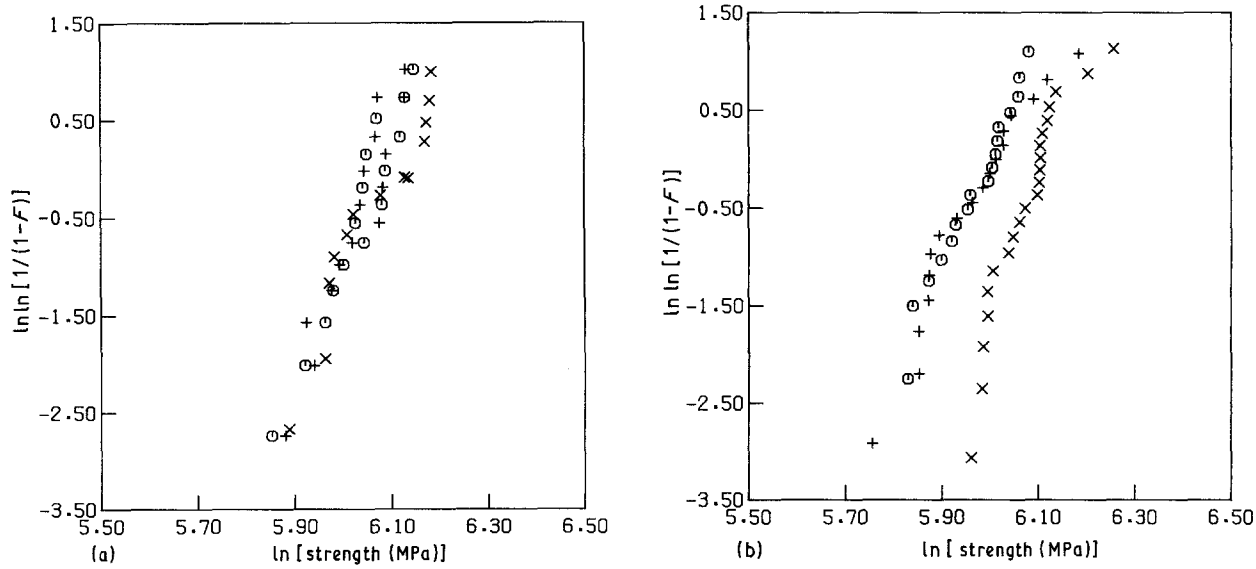

Figure 6 Linearized Weibull plot showing the effect of different static stress levels on the strength distribution after exposure for (a) 1 h, (b) 20 h, (◒) zero-stress, (+) 130 MPa, (x) 265 MPa.

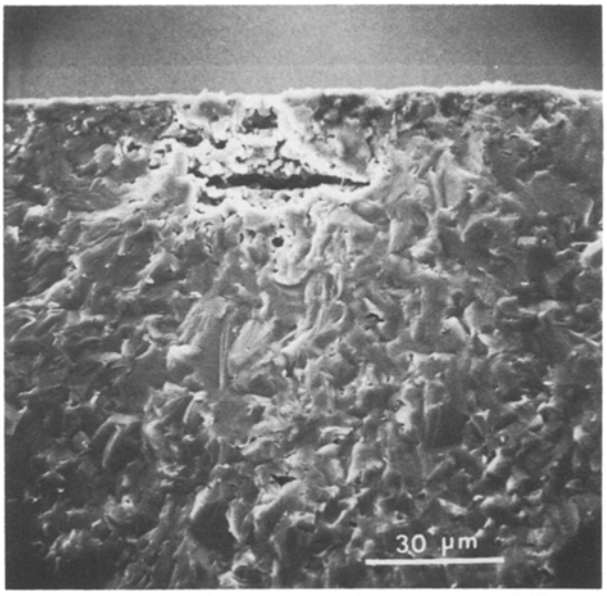

Figure 7 Scanning electron micrograph of a typical failure origin after 20 h exposure under 130 MPa stress: a near-surface pore.

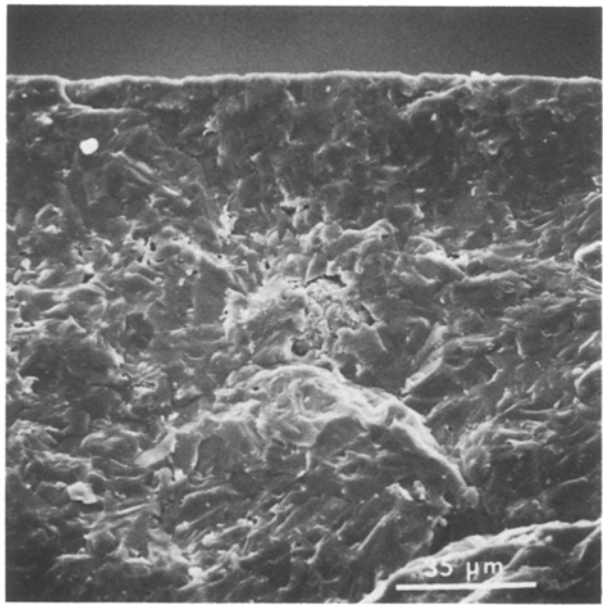

Figure 8 A typical failure origin after 20 h exposure under 265 MPa stress: incomplete sintering.

strengths at all probabilities of failure, showing a strengthening behaviour when compared to the distribution belonging to those specimens exposed to hydrogen for 20 h without stress. This behaviour clearly shows the existence of a stress-dependent strengthening mechanism. The average strength was 436 MPA, 49 MPa more than that after zero-stress exposure. The distribution was also tighter with a Weibull modulus of about 14. A correlation coefficient of 0.93 still indicates a good fit to the two-parameter Weibull distribution. Analysis of variance and SNK tests determined that the average strengths were statistically different, $\bar{S}_0 = \bar{S}_{130} \neq \bar{S}_{265}$.

Failure origins were determined to be surface and/or near-surface pores after 20 h exposures under 130 MPa stress, while after exposures under 265 MPa the stress failures originated mostly from inclusions, loosely sintered regions and from subsurface pores rather than surface-related pores (Fig. 8).

When the strength distributions after 1 h and 20 h exposures under 130 MPa applied stress are compared it is evident that the strength distribution after 20 h exposure is shifted to lower strengths at all probability-of-failure levels. This is the same behaviour as displayed by the corresponding distributions without applied stresses. This indicates that the reaction of hydrogen with the material under lower applied stress is the dominant strength-controlling mechanism. Chemical reactions between hydrogen and specimen surfaces result in the creation of new flaws and the growth of the pre-existent ones, and leads to weakening. This is a time-dependent mechanism because of its chemical nature. The longer the exposure time the more surface deterioration occurs, causing further reduction in strength.

When the strength distributions after exposures under 265 MPa applied stress are compared, the whole distribution is shifted to higher strengths after 20 h exposure. This is contrary to that after zero-stress exposures which shifted to lower strengths. From this observation it is evident that there exists a stress-dependent strengthening mechanism or mechanisms, operating over a certain stress threshold. Similar types of strengthening mechanism have been shown to operate in sintered alpha silicon carbide in air by Easler *et al.* [5], in siliconized silicon carbide by Carroll and Tressler [26], and by Cohrt *et al.* [27]. The strengthening process can be attributed to

(i) Flaw blunting and the stress relaxation process around the crack tip in the high-stress region (localized creep deformation). Relaxation of stresses at the crack tip during high-temperature exposure under static loading would produce compressive stresses at the flaw tip upon unloading and cooling, and this an effective strengthening. Localized deformation at the flaw tip due to the presence of high stress levels may also be responsible for the strengthening behaviour because of its flaw blunting effect.

(ii) Macroscopic stress redistribution in the bending beam through a diffusional creep. Under static stress, due to a creep process (most likely a diffusional creep), a stress redistribution occurs in the bending beam when the material behaviour is non-linear. This effect results in the generation of residual stresses in the beam upon unloading and/or cooling. If the specimens were unloaded after static loading and cooled to room temperature, a residual compressive stress would develop on the tensile side of specimen resulting in a strengthening behaviour. A residual tensile stress would also develop on the compressive side.

4. Summary

The effect of hydrogen on the strength of sintered alpha silicon carbide under different static stress levels at 1370° C was investigated. Exposures to hydrogen causes rapid surface degradation accompanied by a reduction in the strength. Microscopic studies showed that exposures to hydrogen caused delineation of SiC grains. This is thought to be due to preferential

reaction between hydrogen and high-energy grain boundaries. The strengthening and weakening behaviours displayed by sintered alpha silicon carbide are discussed in terms of several mechanisms, i.e. stress relaxation, macrostress redistribution and chemical reactions. These mechanisms may change depending upon the environmental and loading conditions, and probably occur simultaneously, and therefore are in competition to control the overall strength behaviour. Hydrogen can react with the material and change flaw populations, causing weakening, while stress-activated mechanism(s) can lead to strengthening. During the stressed exposures the strength distribution is controlled by the competing mechanisms. Under the lower applied stress (130 MPa), the material showed a weakening behaviour similar to the zero-load exposures for all exposure times. The higher applied stress resulted in a strengthening behaviour for all exposure times. While the cause of this behaviour cannot be explained on the basis of the present data, an analysis of several mechanisms based on stress relaxation, macrostress redistribution, and chemical reaction concepts is provided. These may be regarded as hypotheses for further work.

Fractographic studies of those specimens after exposures with or without applied stress showed that failure originated from the surface and/or subsurface flaws including pores, inclusions and loosely sintered regions which are induced by processing, for all cases studied. The stronger specimens usually failed from subsurface flaws, while weaker ones failed at large surface-related pores. This observation is not different from that of the as-polished control group. It does not therefore lend itself to any obvious conclusions about the effect of hydrogen on the nature of strength-controlling flaws.

References

1. D. C. LARSEN, "Ceramic Materials for Advanced Heat Engines" (Noyes, Park Ridge, 1985) p. 16.
2. B. D. FOSTER, in "Ceramics in Heat Exchangers" edited by B. D. Foster and J. B. Patton (American Ceramic Society, Columbus, 1985) p. 255.
3. "Ceramic Materials for Fusion Reactors", EPRI AP-2515, RP992 (Palo Alto, CA, 1982).
4. E. T. EASLER, MSc thesis, Pennsylvania University (1980).
5. E. T. EASLER, R. E. TRESSLER and C. R. BRADT, *J. Amer. Ceram. Soc.* **64** (1981) 731.
6. C. S. SINGHAL, *Ceram. Int.* **2** (1976) 123.
7. F. F. LANGE, *J. Amer. Ceram. Soc.* **53** (1970) 290.
8. A. J. COSTELLO, R. E. TRESSLER and T. S. I. TSONG, *ibid.* **64** (1981) 332.
9. C. S. COSTELLO and R. E. TRESSLER, *ibid.* **64** (1981) 327.
10. C. S. SINGHAL, *J. Mater. Sci.* **11** (1976) 1246.
11. H. CAPPELEN, H. K. JOHANSEN and K. MOTZFELDT, *Acta Chem. Scand.* **A35** (1981) 247.
12. L. F. HORN, A. J. FILLO and R. J. POWELL, *J. Nucl. Mater.* **85/86** (1979) 439.
13. W. D. McKEE and D. CHATTERJI, *J. Amer. Ceram. Soc.* **59** (1976) 441.
14. K. VERGHESE, R. L. ZUMWALT and P. C. FENG, *J. Nucl. Mater.* **85/86** (1979) 1161.
15. A. R. CAUSEY, J. D. FOWLER and K. ROWANBAKHT, *J. Amer. Ceram. Soc.* **61** (1978) 221.
16. G. S. FISCHMAN, PhD thesis, University of Illinois (1985).
17. P. D. JERO, MSc thesis, University of Illinois (1985).
18. M. J. HARRIS, C. H. GATOS and A. F. WITT, *J. Electrochem. Soc.* **116** (1969) 380.
19. M. KUMAGAWA, H. KUWABARA and S. YAMADA, *Jap. J. Appl. Phys.* **8** (1969) 421.
20. M. J. HARRIS, C. H. GATOS and A. F. WITT, *J. Electrochem. Soc.* **118** (1971) 338.
21. S. MINAGAWA and C. H. GATOS, *Jap. J. Appl. Phys.* **19** (1971) 844.
22. K. V. BURY, "Statistical Models in Applied Science" (Wiley, New York, 1975) p. 273.
23. D. G. S. DAVIES, *Proc. Br. Ceram. Soc.* **22** (1973) 429.
24. C. A. JOHNSON, in "Fracture Mechanics of Ceramics 5" edited by R. C. Bradt, D. P. H. Hasselman and F.F. Lange (Plenum, New York, 1983) p. 365.
25. SPSS/PC+ A comprehensive statistical analysis software package for IBM.PC (SPSS Inc., Chicago, 1986).
26. F. D. CARROLL and R. E. TRESSLER, *J. Amer. Ceram. Soc.* **68** (1985) 143.
27. H. COHRT, G. GRATHWOHL and F. THUMMLER, "Creep and Fracture of Engineering Materials and Structures", Part I (Pineridge, Swansea, 1984) p. 515.

Received 15 June 1987
and accepted 27 January 1988